**13.5**

# GREENLAND AND LABRADOR SEA CONVECTION IN AN OCEAN SEA ICE SIMULATION 1948-2002

Rüdiger Gerdes*, Jörg Hurka, and Michael Karcher

Alfred Wegener Institute for Polar and Marine Research, Bremerhaven, Germany

## 1. INTRODUCTION

Open ocean deep convection in the high latitude North Atlantic is regarded as an important process in the formation of North Atlantic Deep Water. Convection depth varies spatially and temporarily. Deep convection has been observed to occur in the Greenland and Labrador seas. Convection in these areas is not simultaneous but has been described as a seesaw where deep convection in the Labrador Sea is associated with weak convection in the Greenland Sea and vice versa. These differences have been linked to the North Atlantic Oscillation (NAO; Dickson et al., 1996). Deep water production in the Labrador Sea has been intense during the recent period of high index states of the NAO (e.g. Joyce et al., 2000). On the other hand, deep convection in the Greenland Sea has ceased in the late 1970s (Rhein, 1991; Schlosser et al., 1995.). In recent years, small areas of apparent deep convection have been found repeatedly in the Greenland Sea (Gascard et al., 2002) with the hydrographic signature of the convection reaching down to approximately 3000m. In this note, we use results from a ocean-sea ice model of the subpolar North Atantic and the Arctic Ocean as well as atmospheric reanalysis data to assess the variability of convection in the Greenland and Labrador seas over the last 50 years and its relation to the atmospheric forcing.

## 2. MODEL DESCRIPTION AND ANALYSIS

The model used here is based on the MOM-2 model of the GFDL (Pacanowski, 1995). It is formulated on a spherical grid that here has been rotated to avoid excessive zonal resolution near the Pole. The horizontal grid distance is 0.25$^{o}$ in both directions, giving almost uniform resolution of 28 km over the model domain. The vertical is resolved with 30 unevenly spaced levels. We use the FCT advection scheme for tracers. Biharmonic friction is employed while the only diffusion action on tracers is due to the small implicit diffusion of the advection scheme. The ocean model is coupled to a dynamic-thermodynamic

* Corresponding author address: Rüdiger Gerdes, Alfred Wegener Institute, Bussestr. 24, 27750 Bremerhaven, Germany; e-mail: rgerdes@awi-bremerhaven.de

sea ice model with viscous-plastic rheology (Hibler, 1979). The implementation follows that of Harder (1996). The models are coupled following the procedure devised by Hibler and Bryan (1984).

The model has an open boundary at approximately 50°N where the barotropic transport is prescribed from a coarser resolution version of the model that covers the whole Atlantic (Köberle and Gerdes, 2003). At inflow points, temperatures and salinities are taken from the same model. Outflow of tracers and outward propagation of waves is allowed without restrictions.

Forcing of the model is provided by atmospheric fields taken from the NCEP/NCAR reanlysis, however, precipitation and cloudiness are taken from climatology. Standard bulk formulas are used to compute heat fluxes. Initial conditions are from the PHC atlas of Steele et al. (2001). More details are given in Karcher et al. (2003) and Köberle and Gerdes (2003).

Convection depth is diagnosed in the model as the depth where the potential density exceeds the surface density by a fixed, small amount. Inspection of spatial distributions for the winter months during the NCEP Period 1948-2001 revealed a large variability from year to year as well as on longer time scales. During the earlier decades, the Greenland Sea stands out due to the extreme depth of convection but also because of the extreme localization of deep convection to the interior of the Greenland Sea. Convective mixing in the subpolar Atlantic is wide spread although depths are restricted to typically less than 1000m. The same is true for the outer areas of the Norwegian Atlantic Current. Labrador Sea convection apparently occurred in the path of the boundary current that grew gradually denser on its way into and around the Labrador Sea. Deep convection in the Labrador Sea occupies a relatively large area compared to the Greenland Sea.

The indices of convective activity for both regions shown in **Fig.1** are constructed as the

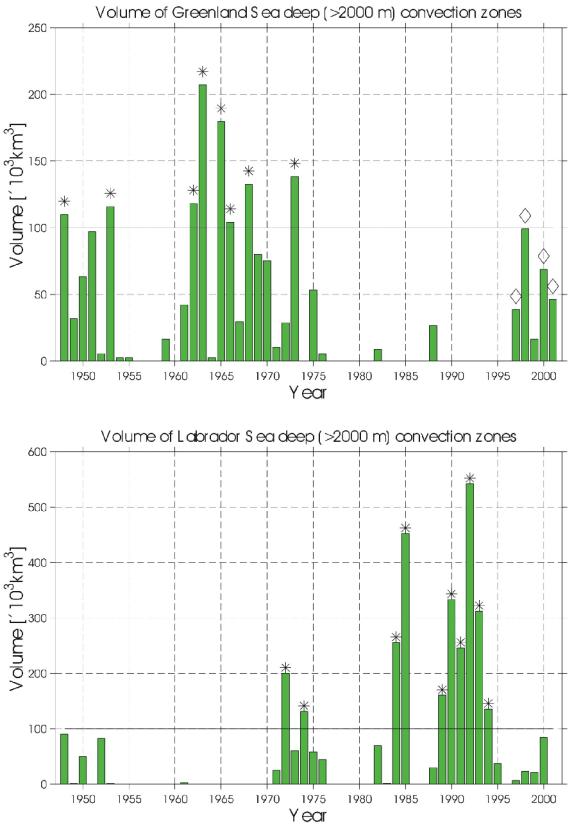


**Figure 1. Convection indices for the Greenland Sea (upper) and the Labrador Sea (lower) based on the volume of convectively**

**mixed water below 2000m depth. Stars indicate winters that have been used to construct composites. A separate composite was build for the three years with deep Greenland Sea convection in the 1990s.**

volume of water below 2000m depth that is convectively mixed during the winter (Jan-April). The years marked with stars in Fig.1 are used to construct composites for strong convection. Those years that show no convective mixing below 2000m at all are used to construct composites for weak convection. Convection in the Greenland Sea is strong between 1960 and the early 1970s. After 1975 there are two decades of basically no deep convection. Only in the second half of the 1990s do we see in the model a recurrence of convection in the Greenland Sea that goes below 2000m depth. The Labrador Sea convection becomes deep in the 1970s and pronounced convective activity is present between 1985 and 1995. This is consistent with the notion of a seesaw between Greenland and Labrador sea convection.

## 3. COMPOSITES

Convection in the Labrador Sea is well correlated with the NAO while the anti-correlation for the Greenland Sea breaks down in the late 1990s where the model produces deep convection despite consistently high positive NAO index values. The composites for sea level pressure (not shown) confirm the relation of the Labrador Sea convection with the NAO. Strong convection is associated with a strong Icelandic low that extends into the Labrador Sea and far north over the Nordic Seas into the Barents Sea. The SLP pattern for weak Greenland Sea convection shows a similar, however, less pronounced pattern. Strong convection in the Greenland Sea and weak convection in the Labrador Sea again have similar SLP patterns associated with them. One noteworthy difference, however, is a shallow low pressure region between Norway and Spitzbergen as well as very high pressure over Greenland in the case of strong Greenland Sea convection. This pattern would allow a large Fram Strait ice export, something that happened in the late 1960s and did not, to all our knowledge, affect convection in the Greenland Sea. In the model we note that the ice that was exported from the Arctic during that time was carried southward along the east Greenland coast without considerable melting and without being diverted into the interior of the Nordic Seas. Strong melting only set in south of Denmark Strait, where it encountered the warm Atlantic waters of the Irminger Current.

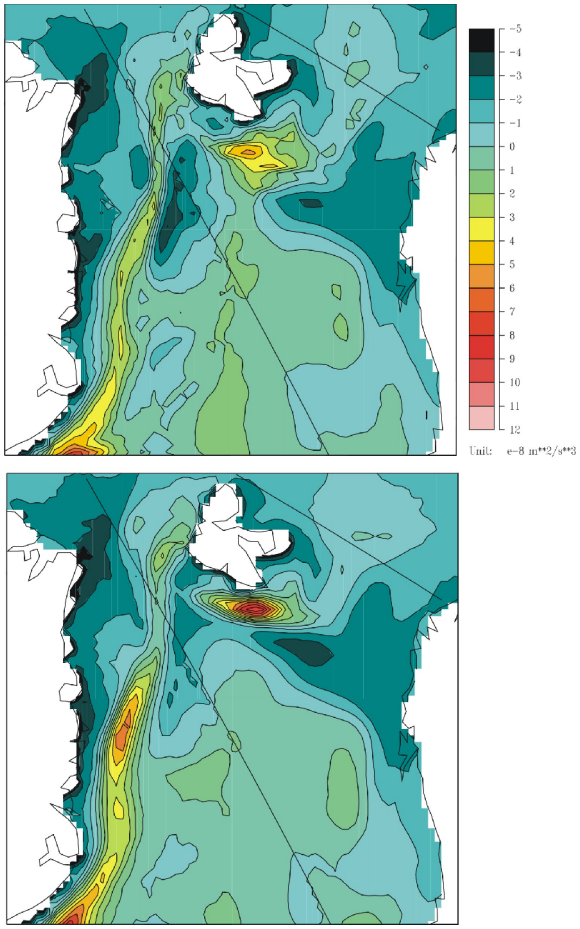


**Figure 2. Surface buoyancy flux in the Greenland Sea for strong convection (upper) and weak convection (lower) composites.**

Strong convection in the Greenland Sea is characterized by strong buoyancy loss in the northern parts of the Greenland Sea. Buoyancy gain in the East Greenland Current remains relatively low and the area of buoyancy gain adjacent to the Greenland Sea is narrow (Fig.2). Also in the Labrador Sea, regions of buoyancy gain and buoyancy loss are close together. In the case of strong convection, a dipol of anomalous surface buoyancy flux exists with gain enhanced at the western and northern rim of the Labrador Sea and loss enhanced in the interior of the basin. This indicates that sea ice edge processes are important in generating the surface flux pattern. Somewhat surprisingly, the sea ice edge in the strong Labrador Sea convection composite lies farther inside the Labrador Sea than in the weak convection composite. However, this is not a closed sea ice cover, the concentration is typically less than 0.3 and the heat loss in the area is strong. In the Greenland Sea strong convection composite sea ice cover is also larger than for the weak convection composite with maximum concentrations reaching 0.75 in the Odden and over 0.95 over the east Greenland shelf. Sea ice cover in the Barents Sea at the same time is relatively small. Thermodynamic growth of sea ice is larger than normal in the northern Greenland Sea. Correspondingly, large negative growth rates occur in the southern part. Melting in the West Spitzbergen Current is large while it is small along the outer edge of the East Greenland Current. This is consistent with the patterns in the surface buoyancy flux. In fact, it can be shown that the buoyancy flux in the Greenland Sea is dominated by the fresh water

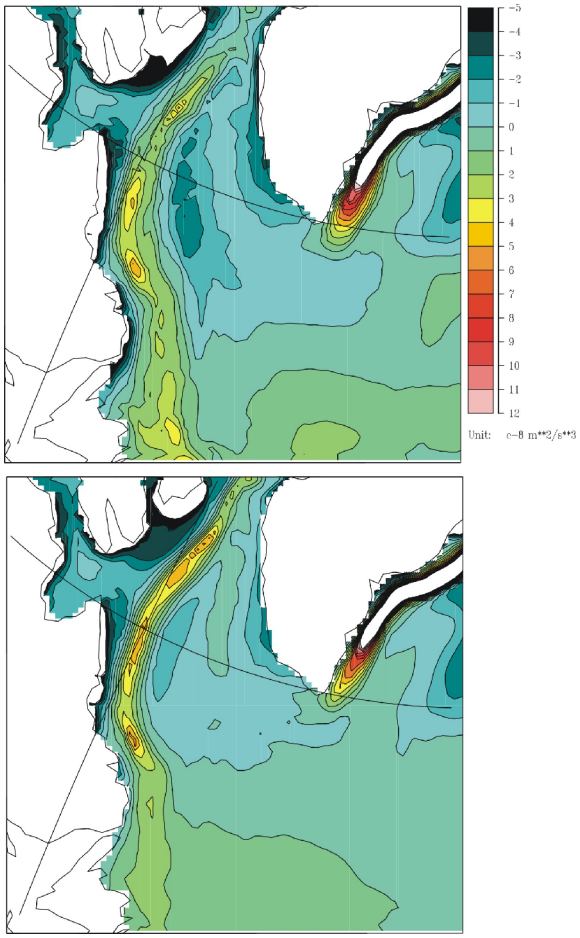


**Figure 3. Surface buoyancy flux in the Labrador Sea for strong convection (upper) and weak convection (lower) composites.**

flux contribution which, in turn, is governed by the thermodynamic growth rate of sea ice. Anomalously large net freezing in the northern Greenland Sea and melting in the southern part requires a transport of sea ice from the north to the south. The differences in wind stress for strong and weak convection periods, respectively, contain subtle but significant differences that lead to higher southward velocities in the interior of the Greenland Sea for the strong convection case. Otherwise we see a stronger cyclonic atmospheric circulation over the whole Nordic Seas, consistent with the surface pressure field. This is associated with a pronounced southward sea ice velocity in the East Greenland Current but smaller velocities farther out in the Greenland Sea.

The strong convection composite for the Labrador Sea also features the stronger cyclonic circulation over the Nordic Seas and a stronger sea ice export from the Arctic that is channelled with the East Greenland Current into the subpolar Atlantic. Melting of sea ice is relatively high off southeast Greenland. Melting conditions occupy a large part of the Labrador Sea and the surface fresh water flux actually opposes convection by increasing the surface buoyancy. Clearly, the changes in heat flux between weak and strong convection are large in the Labrador Sea (more than 200W/m$^2$ difference) and dominate the buoyancy flux changes.

## 4. CONCLUSIONS

Deep convection in the Greenland Sea is highly localized, the surrounding areas are rather stably stratified. The seesaw between Greenland Sea and Labrador Sea convection is reproduced in the model hindcast and deep convection in the Greenland Sea ceases in the model in the late 1970s. Deep convection in the Labrador Sea is related to the NAO and is mainly caused by low air temperatures, the corresponding fresh water flux anomaly tends to hinder convection. The buoyancy flux associated with convection is governed by fresh

water fluxes in the Greenland Sea and by heat fluxes in the Labrador Sea. The fresh water flux in the Greenland Sea that is associated with changes in convection is due to melting and freezing of ice. Deep convection in the Greenland Sea apparently occurs for negative NAO phase. Nevertheless, our composites show a strong pressure gradient over Fram Strait. Ice export from the Arctic is thus relatively large, however, the melting is delayed to lower latitudes, near Denmark Strait. The reoccurrence of deep convection in the 1990s during a high NAO phase is caused by local sea ice growth and drift conditions that are similar to those of the 1960s. Convection occurs in the few years in the 1990s where sea ice extent is relatively large in the Greenland Sea.

**Acknowledgements**: NCEP reanalysis data were provided by the NOAA_CIRES Climate Diagnostics Center, Boulder, Colorado from their Web site at www.cdc.nooa.gov. Partial funding for this work was provided by the European Union project CONVECTION (EVK2-CT-2000-00058) and by the National Science Foundation under agreement no. OPP-0002239 with the International Arctic Research Center, University of Alaska, Fairbanks (Arctic Ocean Model Intercomparison Project).

**References**

Dickson, R.R., J.Lazier, J.Meincke, P.Rhines, and J.Swift, 1996: Long-term coordinated changes in the convective activity of the North Atlantic, Progress in Oceanography, **38**, 241-295

Gascard, J.-C., A.J. Watson, M.-J.Messias, K.A.Olsson, T. Johannessen, K. Simonsen, 2002: Long-lived vortices as a mode of deep ventilation in the Greenland Sea, Nature, **416**, 525 - 527

Harder, M., 1996: Rauhigkeit und Alter des Meereises in der Arktis - Numerische Untersuchungen mit einem großskaligen Modell. Berichte zur Polarforschung, 203, Alfred-Wegener-Institut. (Ph. D. thesis, in German with English summary.)

Hibler, W.D., 1979: A Dynamic Thermodynamic Sea Ice Model. J. Phys. Oceanogr., 9, 815-846.

Hibler, W. D. and K. Bryan, 1987: A Diagnostic Ice-Ocean Model. J. Phys. Oceanogr., 17, 987-1015.

Joyce, T.M., C.Deser, and M.A.Spall, 2000: The relation between decadal variability of subtropical mode water and the North Atlantic Oscillation, J.Climate, 13, 2550-2569

Karcher, M.J., R. Gerdes, F. Kauker, and C. Köberle, 2003: Arctic warming - evolution and spreading of the 1990s warm event in the Nordic Seas and the Arctic Ocean, J.Geophys.Res., **108**, doi:10.1029/2001JC001265

Köberle, C., and R. Gerdes, 2003: Mechanisms determining variability of Arctic sea ice conditions and export, J.Climate (in press).

Pacanowski, R.C., 1995: MOM 2 documentation, user's guide and reference manual, GFDL Ocean Group Tech. Rep. 3, Geophysical Fluid Dynamics Laboratory, Princeton University, Princeton, NJ

Rhein, M., 1991: Ventilation rates of the Greenland and Norwegian Sea derived from distributions of the chlorofluoromehtanes F11 and F12, Deep Sea Research, **38**, 485-503

Schlosser, P., G.Bönisch, B.Kromer, H.H.Loosli, B.Buhler, B.Bayer, G.Bonani, and K.P.Koltermann, 1995: Mid-1980s distribution of tritium, 3He, 14C and 39Ar in the

Greenland/Norwegian seas and the Nansen Basin of the Arctic Ocean: Implications for large-scale circulation patterns, Progress in Oceanography, **35**, 1-28

Steele, M., R.Morfley, and W.Ermold, 2001: PHC: A global ocean hydrography with a high-quality Arctic Ocean, J. Climate, **14**, 2079-2087